Experiment on laser interaction with a planar target for conditions relevant to shock ignition

2014 Phys. Scr. 2014 014017

(http://iopscience.iop.org/1402-4896/2014/T161/014017)

Phys. Scr. T161 (2014) 014017 (4pp) doi:10.1088/0031-8949/2014/T161/014017

Experiment on laser interaction with a planar target for conditions relevant to shock ignition

Y Maheut[1], L Antonelli[1,2], S Atzeni[3], J Badziak[4], F Baffigi[5], D Batani[1], C Cecchetti[5], T Chodukowski[4], F Consoli[6], G Cristoforetti[5], R De Angelis[6], G Folpini[7], L A Gizzi[5], Z Kalinowska[4], M Kucharik[8], P Köster[5], E Krousky[9], L Labate[5], T Levato[2,5], R Liska[8], G Malka[1], A Marocchino[3], P Nicolaï[1], T O'Dell[10], P Parys[4], T Pisarczyk[4], P Rączka[4], O Renner[9], Y J Rhee[11], X Ribeyre[1], M Richetta[2], M Rosinski[4], L Ryć[4], J Skala[9], A Schiavi[3], G Schurtz[1], M Smid[9], C Spindloe[10], J Ullschmied[12], J Wolowski[4] and A Zaraś[4]

[1] Université de Bordeaux, CNRS, CEA, CELIA (Centre Lasers Intenses et Applications), UMR 5107, F-33405 Talence, France
[2] University of Rome 'Tor Vergata', Roma, Italy
[3] Dipartimento SBAI, University of Rome 'La Sapienza' and CNISM, Rome, Italy
[4] Institute of Plasma Physics and Laser Microfusion, Warsaw, Poland
[5] Intense Laser Irradiation Laboratory, INOCNR, Pisa, Italy
[6] Associazione ENEA-Euratom sulla Fusione, Frascati, Italy
[7] University of Milano-Bicocca, Milan, Italy
[8] Czech Technical University, FNSPE, Prague, Czech Republic
[9] Institute of Physics, Prague, Czech Republic
[10] Scitech Precision, Rutherford Appleton Laboratory, Chilton, Didcot, Oxon, UK
[11] Nuclear Data Center, KAERI, Korea
[12] Institute of Plasma Physics ASCR, Prague, Czech Republic

E-mail: maheut@celia.u-bordeaux1.fr

Received 20 September 2013
Accepted for publication 29 November 2013
Published 2 May 2014

Abstract

We report the experiment conducted on the Prague Asterix Laser System (PALS) laser facility dedicated to make a parametric study of the laser–plasma interaction under the physical conditions corresponding to shock ignition thermonuclear fusion reactions. Two laser beams have been used: the auxiliary beam, for preplasma creation on the surface of a plastic foil, and the main beam to launch a strong shock. The ablation pressure is inferred from the volume of the crater in the Cu layer situated behind the plastic foil and by shock breakout chronometry. The population of fast electrons is analyzed by Kα emission spectroscopy and imaging. The preplasma is characterized by three-frame interferometry, x-ray spectroscopy and ion diagnostics. The numerical simulations constrained with the measured data gave a maximum pressure in the plastic layer of about 90 Mbar.

Keywords: laser, plasma, shock ignition, hot electron, shock

(Some figures may appear in color only in the online journal)

1. Introduction

Shock ignition (SI) is a new scheme promising to achieve inertial confinement fusion, thanks to its relative simplicity and the fact that it needs less energy than conventional hot spot schemes [1–3]. In this approach, the target is first compressed at a laser intensity $I < 10^{15}$ W cm^{-2} and then ignited by a strong shock having a pressure greater than 300 Mbar. This scheme potentially has a higher gain and can be tested with the existing laser technology.

However, the laser spike intensity needed for ignition is above the threshold for the nonlinear interaction of the laser beam with a plasma. The interaction is mostly driven by stimulated Brillouin scattering (SBS), stimulated Raman scattering (SRS), two plasmon decay (TPD) and filamentation instabilities that can increase the fraction of reflected light and generate longitudinal electron plasma waves and suprathermal electrons [4, 5]. These electrons can preheat the fuel and reduce the shock pressure if they are too energetic. However, electrons with energy below 100 keV may increase the ablation pressure and thus can be beneficial for shock generation [6, 7].

Here, we present the results of an experiment with intensities in the range 10^{15}–10^{16} W cm^{-2} required for shock ignition. Our goal is to study the influence of the presence of a preplasma corona on laser beam absorption and on shock generation. We also evaluate the effect of laser–plasma instabilities in this range of intensities on the hot electron generation and their influence on shock pressure.

2. Experiment

The experiment was performed at the Prague Asterix Laser System (PALS) kilojoule iodine gas laser. We used three beams: the main beam delivering up to 250 J (3ω, $\lambda = 0.438\,\mu$m, 9×10^{15} W cm^{-2}, 250 ps), an auxiliary beam delivering up to 60 J (1ω, $\lambda = 1.315\,\mu$m, 7×10^{13} W cm^{-2}, 250 ps) and a frequency-doubled probe beam at 657 nm. The first beam having a Gaussian shape focal spot with full-width at half-maximum of 100 μm created a strong shock, while the auxiliary beam having a nearly flat top with 900 μm diameter created an extended preplasma. Phase plates have been used on both beams in order to produce a homogeneous spatial profile. The delay between the two beams has been varied between 0 and 1200 ps.

The choice of targets depends on the diagnostic we wanted to perform. The first one was a multilayer target with 25 μm of Cl doped plastic (C_8H_7Cl, parylene-C) for x-ray spectroscopy, 5 μm of Cu layer for the hot electron detection and 25 μm of Al at the rear side of the target. In some targets, an additional 10 μm layer of Al having a step shape was used to determine the average shock velocity by shock chronometry. Another target with 25 or 40 μm of CH and a thick layer of Cu (a few mm) was used to detect hot electrons and the crater characteristics (volume and shape).

3. Diagnostics

Several complementary diagnostics have been used in the experiment. The first one is three-frame optical interferometry used to characterize the plasma created by the auxiliary beam and the interaction with the main beam. This system uses the frequency-doubled probe beam at 657 nm and provides the plasma size at different times. We also measured the average electron temperature of the preplasma by high-resolution x-ray spectroscopy. The spectrometer is based on a spherical mica crystal covering the spectral range of 3.5–4.5 Å needed to record the Cl Heα to Lyα in the fourth order and Heγ to Heη and Lyβ lines in the fifth diffraction order [8].

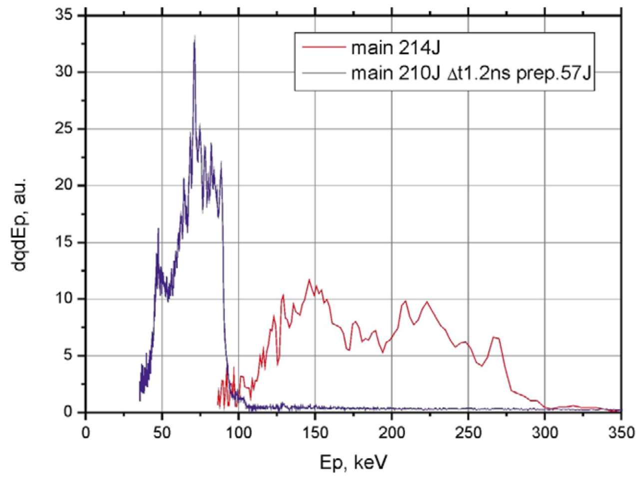

Figure 1. Energy spectra of fast ions (protons) emitted from a plasma produced by irradiation with the main pulse only (red) and by irradiation with both beams at a delay of 1200 ps (blue).

We also performed ion measurements by using eight ion collectors placed at various angles to the target normal and also a SiC detector placed at 30° from the target normal. The first ones were detecting the slow ions and the SiC detector was detecting the fast ions.

The hot electron population was measured from x-ray two-dimensional (2D) images characterizing the Kα emission from the Cu tracer. The imaging system consisted of a spherically bent quartz crystal as a monochromator [9] and films as detectors.

The shock amplitude was studied by two different diagnostics: the shock breakout chronometry and crater measurements. The first one is used for multi-layer targets and measures the thermal self-emission emitted when the shock arrives at the rear side of the target with an optical system and a streak camera. It also detects part of the laser signal used as a reference (fiducial), taken with a beam splitter and brought to the streak camera using an optic fiber.

The second diagnostic is used for thick targets and consists of measuring the volume and the depth of the craters produced in the Cu layer.

4. Results

The characteristics of the preplasma were measured by time-resolved interferometry. The preplasma thickness increases nearly linearly with the expansion time and for the maximum delay between the two beams (i.e. $\Delta t = 1200$ ps), we get a maximum thickness of 0.7 mm, which is of the same order of magnitude as expected in SI experiments.

The temperature of the preplasma and the ablative plasma was measured using an x-ray spectrometer at the target surface [8]. The obtained spectrum is compared with the results of the collisional–radiative PrismSpect code [10]. For the preplasma produced by the auxiliary beam, we obtained a temperature of 175 eV, while for the ablative plasma produced by the main beam we obtained 750 ± 100 eV.

This latter temperature turns out to be practically independent of the preplasma size and the main pulse energy. The temperature of the preplasma is much lower than expected in the plasma corona in SI experiments.

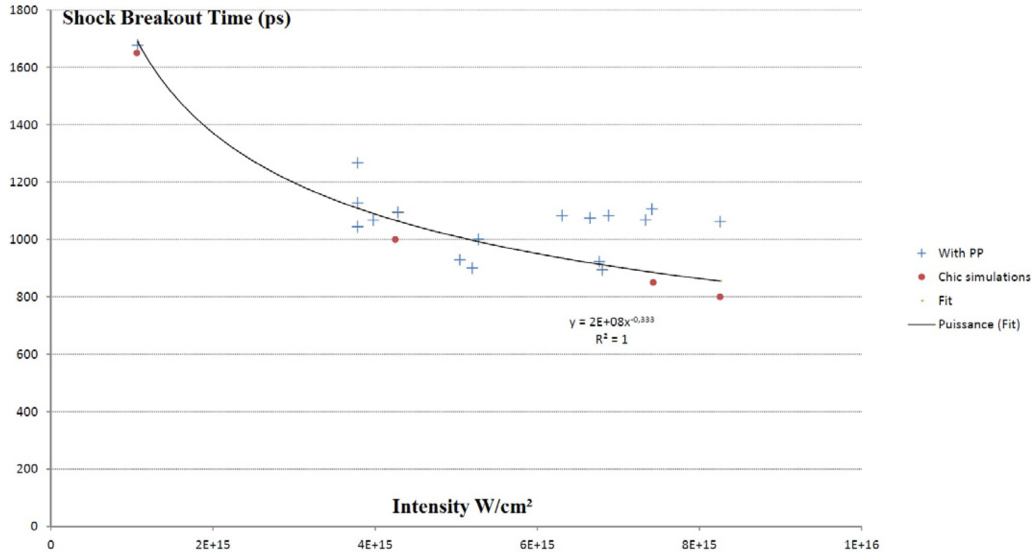

Figure 2. Shock breakout times at the rear side of the multilayer target as a function of the laser main pulse energy.

Considering the emitted ions, the typical spectra obtained (see figure 1) when irradiating the target with the main beam only and with both beams differ dramatically. In the absence of the preplasma (i.e. without the auxiliary beam), we observe ions with energies up to 270 keV, whereas with both beams, the maximum energy is reduced to 90 keV. In both cases, the charge of fast ions represents less than 1% of the total charge of thermal ions. As the fast ions are driven by suprathermal electrons, we conclude that the generation of these electrons is due to different mechanisms of absorption in the two cases. Without preplasma, the resonant absorption is supposed to play a significant role, whereas, with preplasma, the dominant mechanisms are expected to be the parametric instabilities TPD, SRS and SBS. The hot electron temperature was inferred from the proton measurements using the relationship $E_i/A = aT_e$, where E_i is the mean ion (proton here) energy, A is the atomic number and T_e is the electronic temperature that we want to measure. We chose $a = 4.5$ [11, 12] determined from a comparison of the LASNEX code calculations with a set of experimental data from various laboratories [11]. At the energy of the main laser pulse of 200 J, the mean proton energy varied from 80–110 keV (in the presence of preplasma) to 200 keV (in the absence of preplasma), so we could conclude that T_e changes from ∼20 to ∼50 keV [11, 12].

A more direct detection of suprathermal electrons is made by studying the Cu Kα emission using the spherical quartz crystal. We found the dimensions of the hot electron emitting area to be equal to approximately 150 μm for all shots, which is consistent with the focal spot size (100 μm) taking into account the divergent propagation of low-energy suprathermal electrons. We also estimated the penetration depth of the suprathermal electrons using different thicknesses of the plastic layer. Fitting the measured Kα electron flux as a function of the plastic layer thickness with an exponential function, we obtain the penetration depth of 27 μm. Comparing this result with the electron stopping range in mylar (which has a density close to the density of the plastic we used) given in the ESTAR database [13], we deduced that the average hot electron energy is around 50 keV, which is consistent with the ion collector diagnostics. Using the total Kα flux and the mean electron energy, the conversion efficiency into suprathermal electrons was estimated to be below 1%. The suprathermal electrons that we have are, in our regime, mainly due to SRS [14].

The shock pressure was estimated by shock chronometry for multi-layer thin targets and by crater measurements for thick targets. The result of shock chronometry (figure 2) shows that, with the phase plate on the main beam, the shock breakout time follows the scaling law of stationary shocks in the classical regime ($t \propto I^{-1/3}$). However, without the phase plate, we observe very large shot-to-shot fluctuations in the shock breakout time that could be the signature of nonlinear interaction, probably due to non-uniformities in the focal spot.

To deduce the pressure reached in the plastic layer, we performed simulations with the codes DUED [15] and CHIC [16]. The estimated maximum pressure in the plastic layer was 60 Mbar with the phase plate and 90 Mbar without the phase plate. Due to the shock impedance mismatch in the transition between the plastic and other materials, these values correspond, respectively, to 90 and 130 Mbar in Cu and 130 and 210 Mbar in Al.

Nevertheless, in order to reproduce the experimental shock breakout times, we had to reduce the laser intensity in the simulations by a factor of 2. The missing energy could possibly be due to the laser energy refracted outside the cone lens, in particular at large angles with respect to the incident beam (i.e. close to the target surface).

We also measured the characteristics of the crater produced by the shock pressure in Cu (thick targets). Figure 3 shows that the volume of the crater is increasing with the main beam energy. The craters had regular, hemi-spherical shapes with depths from 0.3 mm at $E_{\mathrm{main}} = 50$ J to 0.5 mm at $E_{\mathrm{main}} = 200$ J. As a consequence, the shock pressure is increasing with the main beam energy but is independent of the preplasma thickness within the experimental errors (15–20%). The shock pressure was deduced from the crater measurements by comparing the experimental data with

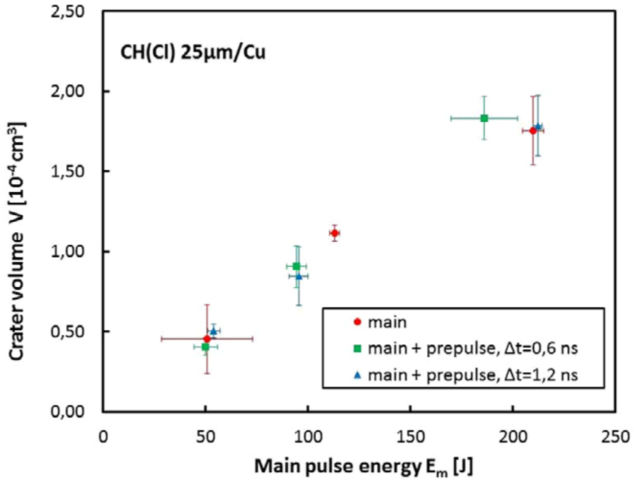

Figure 3. Volume of craters produced in the Cu massive target by the shock wave, induced in the C_8H_7Cl 25 μm layer by the main pulse or by the main pulse with the prepulse, as a function of the main pulse energy. $E_{pre} = 52 \pm 3$ J or 0.

the results of simulations performed with the PALE 2D hydrodynamic code [17]. The maximum pressure inferred in the plastic layer without prepulse is 100 Mbar (82 Mbar with prepulse), but one has to account for a 20% error bar due to the shot-to-shot fluctuation. This pressure is in good agreement with that deduced by shock breakout chronometry.

5. Conclusion

It has been found that the thickness of the preplasma is linearly dependent on the expansion time and that the pressure of the shock does not depend on the preplasma thickness. The conversion efficiency of the laser beam energy to suprathermal electrons is small ($<1\%$) with or without the preplasma and the range of these electrons is approximately 27 μm which corresponds to the average hot electron energy of 50 keV. At intensities in the range of 10^{16} W cm^{-2}, the ablation pressure reached in the plastic layer is about 90–100 Mbar. More data are necessary to understand why the numerical simulations need to use half the incident laser energy to model results corresponding to the experiment. In future experimental campaigns, the preplasma temperature will be increased according to the anticipated SI conditions, which may have a strong impact on the growth rate and saturation of parametric instabilities.

Acknowledgments

The authors acknowledge financial support from the LASERLAB-EUROPE to Research Infrastructure activity within the EC's 7th FP (GA number 284464), from the Czech Ministry MSMT under the grant number LM2010014, from the National Centre for Science (NCN), Poland under the grant number 2012/04/M/ST2/00452, Italian MIUR project PRIN 2009FCC9MS and Sapienza project 2012 C26A12CZH2. The work was conducted within the activities of the Working Package 10 (Fusion experiment) of the HiPER Project.

References

[1] Betti R *et al* 2007 *Phys. Rev. Lett.* **98** 155001
[2] Atzeni S *et al* 2009 *Plasma Phys. Control. Fusion* **51** 124029
[3] Ribeyre X *et al* 2009 *Plasma Phys. Control. Fusion* **51** 015013
[4] Kruer W 1988 *The Physics of Laser Plasma Interaction* (New York: Addison-Wesley)
[5] Klimo O *et al* 2010 *Plasma Phys. Control. Fusion* **52** 055013
[6] Ribeyre X *et al* 2013 *Phys Plasmas* **20** 062705
[7] Guskov S Yu *et al* 2012 *Phys. Rev. Lett.* **109** 255004
[8] Šmid M *et al* 2014 Investigation of x-ray emission induced by hot electrons in dense Cu plasmas *Phys. Scr.* at press
[9] Koch J A *et al* 2003 *Rev. Sci. Instrum.* **74** 2130
[10] MacFarlane J J *et al* 2007 *High Energy Density Phys.* **3** 181
[11] Gitomer S J *et al* 1986 *Phys. Fluids* **29** 2679
[12] Wilks S C *et al* 2001 *Phys. Plasmas* **8** 542
[13] Berger M J *et al* 2012 http://physics.nist.gov/Star
[14] Klimo M 2011 *Phys. Plasmas* **18** 082709
[15] Atzeni S *et al* 2005 *Comput. Phys. Commun.* **169** 153
[16] Breil J *et al* 2011 *Comput. Fluids* **46** 161
[17] Liska R *et al* 2011 *Finite Volumes for Complex Applications VI, Problems & Perspectives* vol 2, ed J Fort *et al* (Berlin: Springer) p 57